

Original Paper

Elastic Buckling Strength of Steel Frames Connected to Core Wall

Kaori NUMABE*, Shosuke MORINO and Jun KAWAGUCHI
(Department of Architecture)

(Received September 17, 2001)

Abstract

An approximate analysis was carried out for the buckling strength of a single-bay multi-story steel frame connected to a core wall. The equilibrium conditions for the member end moments and story shear forces were first expressed in the form of two difference equations containing the rotation angle at each panel point. The difference equations were converted to a set of simultaneous differential equations, by treating the rotation angle as a continuous function. Substituting general solutions for the rotation angle to the differential equations led to a set of homogeneous simultaneous linear equations, and the buckling strength was determined from the condition that the determinant of the coefficient matrix of the simultaneous equations became zero at the instance of the buckling. The size of the coefficient matrix was only 2, and thus the solution was obtained by simple and easy computation. It was shown that the accuracy of the approximate solution was very good, compared with the exact solution obtained by the eigenvalue analysis for several sample frames.

Key Words: steel frame, multi-story, core wall, buckling analysis, approximate solution

1. Introduction

A structural system combining structural walls with steel frames has been employed in the real practice, in which horizontal loads are carried by the walls, and the steel frames carry only vertical loads. The effective length of a framed column in such a wall-frame system is usually taken equal to the story height assuming the lateral sway being prevented by the walls. However, the effective length may be somewhat larger than the story height, since the lateral sway cannot be completely prevented under the work of the horizontal load. This problem has not yet been clarified.

In the course of the structural design of steel frames, the buckling analysis is scarcely performed, and align-

* Aoshima Architects & Engineers, Inc.

ment charts are often used to evaluate the column effective length. The error involved in the application of the alignment charts to an irregular frame has been discussed by Lind(1977) and Cheong-Siat Moy(1978), and Chu and Chou(1969) have suggested a modification of the column effective length applicable to the frames with relatively small irregularities. Wood(1974) presented an exact method of evaluating the buckling strength of a fish-bone-shaped frame (multi-story column restrained by beams at each panel point), utilizing the buckling condition that the summation of the column stiffness reduced by the axial force and the beam stiffness at any arbitrary panel point became zero at the instance of buckling. On the other hand, Sakamoto(1980) presented a method for the modification of the column effective length of a multi-bay single-story frame. In this method, the equilibrium was considered on the deflected frame, in which the column deflection was approximated by a sine shape with a half length equal to the effective length determined from the alignment chart. The methods presented by Wood and Sakamoto are only applicable to a fish-bone-shaped frame or a single-story frame. The authors (Morino, Kawaguchi and Suzuki 1993) combined these two methods, and presented a method to compute approximately the buckling strength of a multi-story multi-bay frame, which first reformed a given frame to a single-bay frame using Sakamoto's idea, and then the buckling strength of the reformed frame was computed by Wood's method. However, this treatment may not be directly applicable to the steel frames with core walls.

The purpose of the research in this paper is to present an approximate method of evaluating the column effective length of a frame with a core wall, and to investigate the accuracy of the approximate solution in view of the exact solution based on the eigenvalue analysis.

2. Approximate Analysis of Frame Buckling

2.1 Description of Model Frame

Figure 1 shows a multi-story single-bay model frame for the buckling analysis. A steel beam-and-column assembly of m -story is pin-connected or rigidly-connected at each beam end to a core wall. The flexural stiffness of

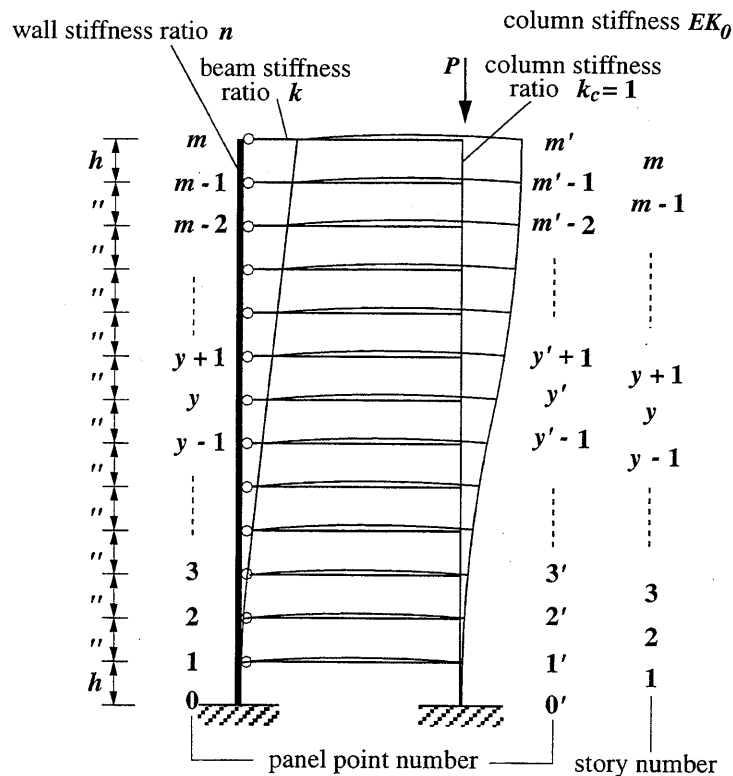


Fig. 1 Frame Model for Analysis

a column is denoted by EK_0 , and the ratio of the lateral stiffness of the core wall to the column stiffness and the ratio of the beam flexural stiffness to the column stiffness are denoted by n and k , respectively. The numbering for the stories and that for the panel points at beam-to-wall connections are given by $1, 2, \dots, y, \dots, m$, and that for the panel points at beam-to-column connections are given by $1', 2', \dots, y', \dots, m'$, as shown in the figure. It is assumed for the simplicity that a single vertical load is applied at the top of the column only, and thus the axial force in the column in each story is constant, and the axial force in the wall is zero. It is also assumed that the values of n, k , the story height h and the column stiffness ratio are all constant along the height of the frame.

The following formulations are made for the frame in which the beam ends are pin-connected to the wall.

2.2 Formulation of Difference Equations

The basic slope-deflection equations for a buckled member are applied to member end moments at the panel points y and y' , and to shear forces in the wall and column of the story y as follows:

$$\begin{aligned}
 M_{y \ y+1} &= nEK_0 (4\theta_y + 2\theta_{y+1} - 6R_{y+1}) & M_{y \ y'} &= 0 \\
 M_{y \ y-1} &= nEK_0 (4\theta_y + 2\theta_{y-1} - 6R_y) & & \\
 M_{y' \ y'+1} &= EK_0 (\alpha\theta_{y'} + \beta\theta_{y'+1} - \gamma R_{y+1}) & M_{y' \ y} &= 3kEK_0\theta_{y'} & (1) \\
 M_{y' \ y'-1} &= EK_0 (\alpha\theta_{y'} + \beta\theta_{y'-1} - \gamma R_y) & & \\
 Q_{y \ y-1} &= -\frac{nEK_0}{h} (6\theta_y + 6\theta_{y-1} - 12R_y) & Q_{y' \ y'-1} &= -\frac{EK_0}{h} (\gamma\theta_{y'} + \gamma\theta_{y'-1} - \delta R_y)
 \end{aligned}$$

The definition of the member end moments M and the shear forces Q , and their positive directions are given in Fig. 2. The rotation at the panel point and the chord rotation of the column are denoted by θ and R , respectively, and their positive direction is clockwise. The parameters α, β, γ and δ are stability functions of the load parameter Z , and they are given as follows:

$$\begin{aligned}
 \alpha &= \frac{Z \sin Z - Z^2 \cos Z}{2(1 - \cos Z) - Z \sin Z} & \beta &= \frac{Z^2 - Z \sin Z}{2(1 - \cos Z) - Z \sin Z} \\
 \gamma &= \alpha + \beta & \delta &= 2\gamma - Z^2 & (2) \\
 Z &= h \sqrt{\frac{P}{EI}} & E &: \text{Young's modulus} & I &: \text{moment of inertia} & h &: \text{story height}
 \end{aligned}$$

The equilibrium of member end moments at the points y and y' and the equilibrium of the story shear of the stories y and $y+1$ give the following equations:

$$\begin{aligned}
 M_{y \ y+1} + M_{y \ y-1} &= 0 & M_{y' \ y'+1} + M_{y' \ y'-1} + M_{y' \ y} &= 0 & (3) \\
 Q_{y \ y-1} + Q_{y' \ y'-1} &= 0 & Q_{y \ y+1} + Q_{y' \ y'+1} &= 0
 \end{aligned}$$

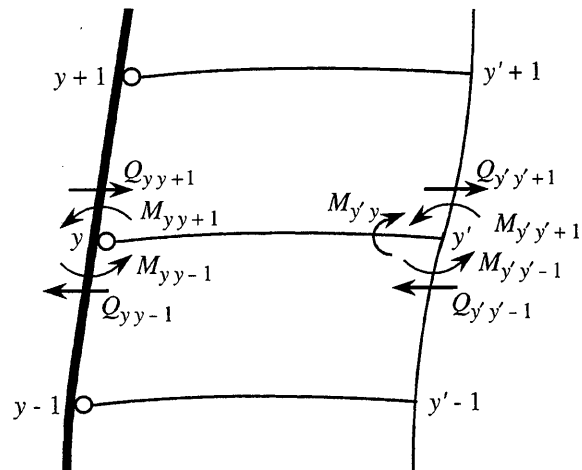


Fig. 2 Member End Moment and Column Shear

The expression of a chord rotation angle in terms of the panel rotation angle is derived by substituting the shear forces in Eq. (1) into the shear equilibrium of Eq. (3), as follows:

$$R_y = \frac{1}{12n + \delta} \{6n(\theta_{y-1} + \theta_y) + \gamma(\theta_{y'-1} + \theta_{y'})\} \quad (4)$$

$$R_{y+1} = \frac{1}{12n + \delta} \{6n(\theta_y + \theta_{y+1}) + \gamma(\theta_{y'} + \theta_{y'+1})\}$$

Substituting Eq. (4) into the equilibrium equations for the member end moments in Eq. (3) leads to

$$\begin{aligned} (2 - \frac{36n}{12n + \delta})(\theta_{y-1} + 2\theta_y + \theta_{y+1}) + 4\theta_y \\ - \frac{6\gamma}{12n + \delta}(\theta_{y'-1} + 2\theta_{y'} + \theta_{y'+1}) = 0 \\ - \frac{6n\gamma}{12n + \delta}(\theta_{y-1} + 2\theta_y + \theta_{y+1}) \\ + (\beta - \frac{\gamma^2}{12n + \delta})(\theta_{y'-1} + 2\theta_{y'} + \theta_{y'+1}) + (2\alpha + 3k - 2\beta)\theta_{y'} = 0 \end{aligned} \quad (5)$$

2.3 Conversion of Difference Equations to Differential Equations

Note that Eq. (5) is a set of difference equations in which the terms

$$X = \theta_{y-1} + 2\theta_y + \theta_{y+1} \quad Y = \theta_{y'-1} + 2\theta_{y'} + \theta_{y'+1} \quad (6)$$

repeatedly appears. Then, Eq. (5) is written as follows:

$$(6n - \delta)X + 3\gamma Y - (24n + 2\delta)\theta_y = 0 \quad (7)$$

$$6n\gamma X - (12n\beta + \beta\delta - \gamma^2)Y - (12n + \delta)(2\alpha + 3k - 2\beta)\theta_{y'} = 0$$

Here, by treating θ_y and $\theta_{y'}$ as continuous functions of y and y' , respectively, finite difference expressions of the second derivative of θ_y and $\theta_{y'}$ with respect to y and y' are given as follows:

$$\frac{d^2 \theta_y}{d y^2} = \theta''_y = \frac{\theta_{y-1} - 2\theta_y + \theta_{y+1}}{a^2} \quad \frac{d^2 \theta_{y'}}{d y'^2} = \theta''_{y'} = \frac{\theta_{y'-1} - 2\theta_{y'} + \theta_{y'+1}}{a^2} \quad (8)$$

where a denotes the size of the subdivided segments, but y and y' are integer numbers, and thus $a = 1$. Then, the terms given by Eq. (6) are written as

$$X = \theta''_y + 4\theta_y \quad Y = \theta''_{y'} + 4\theta_{y'} \quad (9)$$

Substituting Eq. (9) into Eq. (7) leads to

$$\begin{aligned} (6n - \delta)\theta''_y - 6\delta\theta_y + 3\gamma\theta''_{y'} + 12\gamma\theta_{y'} = 0 \\ 6n\gamma\theta''_y + 24n\gamma\theta_y - (12n\beta + \beta\delta - \gamma^2)\theta''_{y'} \\ - 4(12n\beta + \beta\delta - \gamma^2)\theta_{y'} - (12n + \delta)(2\alpha - 2\beta + 3k)\theta_{y'} = 0 \end{aligned} \quad (10)$$

Finally, the equilibrium condition given by Eq. (5) is converted to a set of simultaneous linear differential equations for θ_y and $\theta_{y'}$.

2.4 Buckling Condition and Its Solution

(a) Frame with Pin Connections at Beam Ends

General solution for θ_y and $\theta_{y'}$ of Eq. (10) is given by

$$\theta_y = C_1 \cos \rho y + C_2 \sin \rho y \quad \theta_{y'} = C'_1 \cos \rho' y' + C'_2 \sin \rho' y' \quad (11)$$

The condition that integral constants C_i and C'_i and parameters ρ and ρ' must satisfy is derived by the following manner. First, the fixed condition at the column base; $\theta_0 = \theta_0' = 0$, at $y = y' = 0$, gives $C_1 = C'_1 = 0$, and thus

$$\theta_y = C_2 \sin \rho y \quad \theta_{y'} = C'_2 \sin \rho' y' \quad (12)$$

$$a_{22} = (12n\beta + \beta\delta - \gamma^2)\rho^2 - (12n + \delta)(2\alpha + 2\beta + 3k) + 4\gamma^2$$

The buckling condition is that the determinant of the coefficient matrix of Eq. (19) becomes zero, when the load parameter Z takes the critical value, and thus the buckling condition is given by

$$\begin{vmatrix} a_{11} & a_{12} \\ a_{21} & a_{22} \end{vmatrix} = a_{11} \cdot a_{22} - a_{12} \cdot a_{21} = 0 \quad (21)$$

The buckling load parameter Z_{cr} of the frame shown in Fig. 1 is determined as the smallest value of the load parameter that satisfies Eq. (21). The effective length of the column l_k is given by the formula

$$l_k = \frac{\pi}{Z_{cr}} \quad (22)$$

which is derived by substituting Euler's load expression for the column with length l_k into Z in Eq. (2).

(b) Frame with Rigid Connections at Beam Ends

In the case of the frame in which the beam ends are rigidly-connected to the core wall, the slope-deflection equation for the beam end moments at the panel points y and y' are given as follows:

$$M_{y y'} = kEK_0(4\theta_y + 2\theta_{y'}) \quad M_{y' y} = kEK_0(4\theta_{y'} + 2\theta_y) \quad (23)$$

Using Eq. (23) instead of $M_{yy'} = 0$ and $M_{y'y} = 3kEK_0\theta_{y'}$ in Eq. (1) leads to the following equilibrium equations which corresponds to Eq. (5):

$$\begin{aligned} (2n - \frac{36n^2}{12n + \delta})(\theta_{y-1} + 2\theta_y + \theta_{y+1}) + (4n + 4k)\theta_y \\ - \frac{6n\gamma}{12n + \delta}(\theta_{y'-1} + 2\theta_{y'} + \theta_{y'+1}) + 2k\theta_{y'} = 0 \\ - \frac{6n\gamma}{12n + \delta}(\theta_{y-1} + 2\theta_y + \theta_{y+1}) + 2k\theta_y \\ + (\beta - \frac{\gamma^2}{12n + \delta})(\theta_{y'-1} + 2\theta_{y'} + \theta_{y'+1}) + (2\alpha + 4k - 2\beta)\theta_{y'} = 0 \end{aligned} \quad (24)$$

The procedure to derive the buckling condition is the same as the one shown for the frame with pin connections at the beam ends. The buckling condition is given in the same form as Eq. (21), and four elements are given as follows:

$$\begin{aligned} a_{11} &= (6n^2 - n\delta)(4 - \rho^2) - (12n + \delta)(2n + 2k) \\ a_{12} &= 3n\gamma(4 - \rho^2) - k(12n + \delta) \\ a_{21} &= 6n\gamma(4 - \rho^2) - 2k(12n + \delta) \\ a_{22} &= (\gamma^2 - 12n\beta - \beta\delta)(4 - \rho^2) - (12n + \delta)(2\alpha - 2\beta + 4k) \end{aligned} \quad (25)$$

3. Eigenvalue Analysis of Frame Buckling

3.1 Model Frame A

3.1.1 Description of Model Frame A

Model frame A is the same as the multi-story single-bay frame shown in Fig. 1. The beam ends are pin- or rigidly-connected to the core wall. The flexural stiffness of the column EK_0 , the ratio of the lateral stiffness of the core wall to the column stiffness n , the ratio of the beam flexural stiffness to the column stiffness k , the story height h , and the load parameter Z are all constant along the height of the frame.

3.1.2 Equilibrium Equations

(a) Frame with Pin Connections at Beam Ends

As explained in the previous section, the equilibrium of the member end moments and the story shear given by Eq. (3) are converted to a set of difference equations, Eq. (5). Applying Eq. (5) to $y = 1, 2, 3, \dots, \text{and } m - 1$, and $y' = 1', 2', 3', \dots, \text{and } m' - 1$ leads to a set of $2(m - 1)$ homogeneous equations expressed in terms of $2(m + 1)$ panel point rotation angles, among which the number of unknowns are $2m$ noting that $\theta_0 = \theta_0' = 0$. Additional two equations are obtained by considering the equilibrium at the top floor. Substituting the expression of the member end moments given by Eq. (1) into the member end moment equilibrium at $y = m$ and $y' = m'$, that is, $M_{m\ m-1} = 0$ and $M_{m'\ m'-1} + M_{m'\ m} = 0$, leads to

$$M_{m\ m-1} = nEK_0(4\theta_m + 2\theta_{m-1} - 6R_m) = 0 \quad (26)$$

$$M_{m'\ m'-1} + M_{m'\ m} = EK_0\{(\alpha + 3k)\theta_{m'} + \beta\theta_{m'-1} - \gamma R_m\} = 0$$

Eliminating the chord rotation angles in view of Eq. (4), the equilibrium equations at the panel point m and m' are obtained as follows:

$$\begin{aligned} (2 - \frac{36n}{12n + \delta})\theta_{m-1} + (4 - \frac{36n}{12n + \delta})\theta_m - \frac{6\gamma}{12n + \delta}\theta_{m'-1} - \frac{6\gamma}{12n + \delta}\theta_{m'} = 0 \quad (27) \\ - \frac{6n\gamma}{12n + \delta}\theta_{m-1} - \frac{6n\gamma}{12n + \delta}\theta_m + (\beta - \frac{\gamma^2}{12n + \delta})\theta_{m'-1} + (\alpha + 3k - \frac{\gamma^2}{12n + \delta})\theta_{m'} = 0 \end{aligned}$$

Finally, a set of homogeneous simultaneous equation with the size $2m \times 2m$ is obtained, as shown below.

$$[A]\{\Theta\} = \{0\} \quad (28)$$

where $[A]$ is the coefficient matrix and $\{\Theta\}$ is the unknown vector containing $\theta_1 \sim \theta_m$ and $\theta_{1'} \sim \theta_{m'}$. Each element of the coefficient matrix $[A]$ is a transcendental function of the load parameter Z .

(b) Frame with Rigid Connections at Beam Ends

The equilibrium equations for a general panel points y and y' are already shown by Eq. (24), which corresponds to Eq. (5). Two additional equations corresponding to Eq. (27) are obtained by considering the equilibrium at the top floor, as follows:

$$\begin{aligned} (2n - \frac{36n^2}{12n + \delta})\theta_{m-1} + (4n + 4k - \frac{36n^2}{12n + \delta})\theta_m \\ - \frac{6n\gamma}{12n + \delta}\theta_{m'-1} + (2k - \frac{6n\gamma}{12n + \delta})\theta_{m'} = 0 \quad (29) \\ - \frac{6n\gamma}{12n + \delta}\theta_{m-1} + (2k - \frac{6n\gamma}{12n + \delta})\theta_m \\ (\beta - \frac{\gamma^2}{12n + \delta})\theta_{m'-1} + (\alpha + 4k - \frac{\gamma^2}{12n + \delta})\theta_{m'} = 0 \end{aligned}$$

The final form of the homogeneous simultaneous equations is the same as Eq. (28).

3.2 Model Frame B

In the model frames treated so far, it is assumed that the stiffness of the wall, beams and columns, and the load parameter are all constant along the height of the frame. Then, a question arises: Is the approximate solution applicable to real tall buildings?

The buckling analysis starts with the equilibrium of the member end moments at each panel point, and the shear in each story, and the final form of the simultaneous equation is homogeneous. The equilibrium conditions at a certain panel point and a certain story are quite local, and not affected by the conditions at other panel points and stories that are far apart from the point and the story under consideration. This leads to a hypothesis that the approximate solution is applicable to a frame in which the condition of the constant distribution of the stiffness and

the load parameter is locally satisfied. More precisely, the approximate solution is applicable to a frame which satisfies the following conditions: i) the stiffness ratios of upper and lower columns at each panel point are nearly equal; ii) the stiffness ratios of upper and lower walls at each panel point are nearly equal; iii) the stiffness ratios of upper and lower beams of each story are nearly equal; and iv) the load parameter Z of upper and lower columns at each panel point are nearly equal. It is understood from the definition of Z in Eq. (2) that the condition iv) is satisfied, if the height of each story is nearly equal, and the distributions of the column axial force and the moment of inertia of column section along the height of the frame are similar. In order to investigate the authenticity of this hypothesis, model frame B in which the stiffness and the load parameter are linearly varying along the height is analyzed in the following section.

3.2.1 Description of Model Frame B

Model frame B is the one shown in Fig. 1, but the stiffness and the load parameter are linearly varying along the height. Figure 4(a) shows the distribution of the column stiffness ratio k_{c_y} , where $k_{c_1} = 1$ at the bottom story, and $k_{c_m} = a$ at the top story. At a general story y , the column stiffness ratio is given by

$$k_{c_y} = \frac{1}{m-1} \{m-y+a(y-1)\} \quad (30)$$

The distributions of wall stiffness ratio k_{w_y} and beam stiffness ratio k_{b_y} are assumed to be similar to that for the column, and thus

$$k_{w_y} = n k_{c_y} \quad k_{b_y} = k k_{c_y} \quad (31)$$

The linear distribution is also assumed for the load parameter Z as shown in Fig. 4(b), where $Z_1 = Z$ at the bottom story, and $Z_m = \kappa Z$ at the top story. At a general story y , the load parameter Z_y is given by

$$Z_y = \frac{1}{m-1} \{m-y+\kappa(y-1)\}Z \quad (32)$$

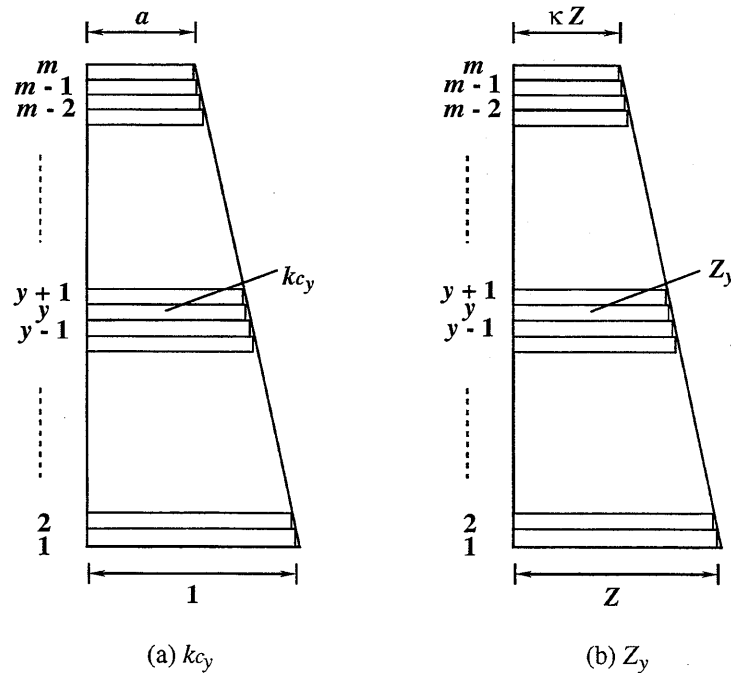


Fig. 4 Distribution of Column Stiffness Ratio k_{c_y} and Load Parameter Z_y

3.2.2 Equilibrium Equations

(a) Frame with Pin Connections at Beam Ends

The expressions for the member end moments and shear forces are as follows:

$$\begin{aligned}
M_{y,y+1} &= kw_{y+1}EK_0 (4\theta_y + 2\theta_{y+1} - 6R_{y+1}) \\
M_{y,y-1} &= kw_yEK_0 (4\theta_y + 2\theta_{y-1} - 6R_y) \\
M_{y,y'} &= 0 \\
M_{y',y'+1} &= kc_{y+1}EK_0 (\alpha_{y+1}\theta_{y'} + \beta_{y+1}\theta_{y'+1} - \gamma_{y+1}R_{y+1}) \\
M_{y',y'-1} &= kc_yEK_0 (\alpha_y\theta_{y'} + \beta_y\theta_{y'-1} - \gamma_yR_y) \\
M_{y',y} &= 3kb_yEK_0\theta_{y'} \\
Q_{y,y-1} &= -\frac{kw_yEK_0}{h} (6\theta_y + 6\theta_{y-1} - 12R_y) \\
Q_{y',y'-1} &= -\frac{kc_yEK_0}{h} (\gamma_y\theta_{y'} + \gamma_y\theta_{y'-1} - \delta_yR_y)
\end{aligned} \tag{33}$$

The parameters α_y , β_y , γ_y and δ_y are stability functions of the load parameter Z_y , computed by Eq. (2). The expressions of chord rotation angles in terms of the panel rotation angles are derived by substituting the shear forces in Eq. (33) into the shear equilibrium of Eq. (3), as follows:

$$R_y = \frac{1}{12kw_y + \delta_y kc_y} \{ 6kw_y(\theta_{y-1} + \theta_y) + \gamma_y kc_y(\theta_{y'-1} + \theta_{y'}) \} \tag{34}$$

$$R_{y+1} = \frac{1}{12kw_{y+1} + \delta_{y+1} kc_{y+1}} \{ 6kw_{y+1}(\theta_y + \theta_{y+1}) + \gamma_{y+1} kc_{y+1}(\theta_{y'} + \theta_{y'+1}) \}$$

Substituting Eq. (34) into the equilibrium equations for the member end moments in Eq. (3) leads to

$$\begin{aligned}
&kw_y(2 - a_y)\theta_{y-1} + \{ kw_y(4 - a_y) + kw_{y+1}(4 - a_{y+1}) \}\theta_y + kw_{y+1}(2 - a_{y+1})\theta_{y+1} \\
&\quad - kw_y b_y \theta_{y'-1} - (kw_y b_y + kw_{y+1} b_{y+1})\theta_{y'} - kw_{y+1} b_{y+1} \theta_{y'+1} = 0 \\
&- kc_y b'_y \theta_{y-1} - (kc_y b'_y + kc_{y+1} b'_{y+1})\theta_y - kc_{y+1} b'_{y+1} \theta_{y+1} \\
&\quad + kc_y(\beta_y - c_y)\theta_{y'-1} - (\alpha_y kc_y + \alpha_{y+1} kc_{y+1} + 3kb_y - kc_y c_y - kc_{y+1} c_{y+1})\theta_{y'} \\
&\quad + kc_{y+1}(\beta_{y+1} - c_{y+1})\theta_{y'+1} = 0
\end{aligned} \tag{35}$$

where

$$\begin{aligned}
a_y &= \frac{36 \frac{kw_y}{kc_y}}{12 \frac{kw_y}{kc_y} + \delta_y} & b_y &= \frac{6\gamma_y}{12 \frac{kw_y}{kc_y} + \delta_y} \\
b'_y &= \frac{6\gamma_y \frac{kw_y}{kc_y}}{12 \frac{kw_y}{kc_y} + \delta_y} & c_y &= \frac{\gamma_y^2}{12 \frac{kc_{y+1}}{kc_y} + \delta_y}
\end{aligned} \tag{36}$$

Equations (35) can be applicable to the panel points $y = 1, 2, 3, \dots, \text{and } m - 1$, and $y' = 1', 2', 3', \dots, \text{and } m' - 1$, in view of $\theta_0 = \theta_{0'} = 0$, and $kc_{m+1} = kw_{m+1} = 0$. Then, a set of homogeneous simultaneous equations with the size $2m \times 2m$ containing $\theta_1 \sim \theta_m$ and $\theta_{1'} \sim \theta_{m'}$ is obtained.

(b) Frame with Rigid Connections at Beam Ends

The expressions for the member end moments and shear forces are given by Eq. (33), except for the beam

end moments, that is,

$$M_{y,y'} = kb_y EK_0 (4\theta_{y'} + 2\theta_y) \quad M_{y',y} = kb_y EK_0 (4\theta_{y'} + 2\theta_y) \quad (37)$$

The equations corresponding to Eq. (35) are given by

$$\begin{aligned} & kw_y(2 - a_y)\theta_{y-1} + \{kw_y(4 - a_y) + kw_{y+1}(4 - a_{y+1}) + 4kb_y\}\theta_y + kw_{y+1}(2 - a_{y+1})\theta_{y+1} \\ & - kw_y b_y \theta_{y'-1} - (kw_y b_y + kw_{y+1} b_{y+1} - 2kb_y)\theta_{y'} - kw_{y+1} b_{y+1} \theta_{y'+1} = 0 \\ & - kc_y b'_y \theta_{y-1} - (kc_y b'_y + kc_{y+1} b'_{y+1} - 2kb_y)\theta_y - kc_{y+1} b'_{y+1} \theta_{y+1} \\ & + kc_y(\beta_y - c_y)\theta_{y'-1} - (\alpha_y kc_y + \alpha_{y+1} kc_{y+1} + 4kb_y - kc_y c_y - kc_{y+1} c_{y+1})\theta_{y'} \\ & + kc_{y+1}(\beta_{y+1} - c_{y+1})\theta_{y'+1} = 0 \end{aligned} \quad (38)$$

3.3 Model Frame C

3.3.1 Description of Model Frame C

Model frame C shown in Fig. 5 is a multi-story single-bay connected to a perfectly rigid wall, and thus the sideway is prevented. The beam ends are pin- or rigidly-connected to the wall. The flexural stiffness of the column EK_0 , the ratio of the beam flexural stiffness to the column stiffness k , story height h , and the load parameter Z are all constant along the height of the frame.

3.3.2 Equilibrium Equations

For the buckling analysis of the frames shown in Fig. 5, it is only needed to consider the equilibrium of the member end moments at the panel points along the column in view of the chord rotation angle R being 0.

(a) Frame with Pin Connections at Beam Ends

At a general panel point y' of the frame shown in Fig. 5(a), the equilibrium is given by $M_{y',y'-1} + M_{y',y} + M_{y',y'+1} = 0$, and substituting the expressions for the member end moments in Eq. (1) in view of $R_{y'} = R_{y'+1} = 0$ leads to

$$\beta\theta_{y'-1} + (2\alpha + 3k)\theta_{y'} + \beta\theta_{y'+1} = 0 \quad (39)$$

At the top floor, the equilibrium becomes $M_{m',m'-1} + M_{m',m} = 0$, and

$$\beta\theta_{m'-1} + (\alpha + 3k)\theta_{m'} = 0 \quad (40)$$

is obtained. A set of m equations, $(m - 1)$ equations obtained by applying Eq. (39) to the panel points $y' = 1', 2', 3', \dots, m' - 1$ and Eq. (40), forms the homogeneous simultaneous equations with the size $m \times m$ similar to Eq. (28), in which $\{\Theta\}$ contains $\theta_{1'} \sim \theta_{m'}$, noting that $\theta_{0'} = 0$.

(b) Frame with Rigid Connections at Beam Ends

For the frame shown in Fig. 5(b), two equations corresponding to Eqs. (39) and (40) are obtained as follows:

$$\beta\theta_{y'-1} + (2\alpha + 2k)\theta_{y'} + \beta\theta_{y'+1} = 0 \quad (42)$$

$$\beta\theta_{m'-1} + (\alpha + 2k)\theta_{m'} = 0 \quad (43)$$

Again, a set of homogeneous simultaneous equations with the size $m \times m$ containing $\theta_{1'} \sim \theta_{m'}$ is obtained.

3.4 Buckling Condition and Its Solution

The final form of the equilibrium equations of a buckled frame is given by Eq. (28), regardless of the model frame consid-

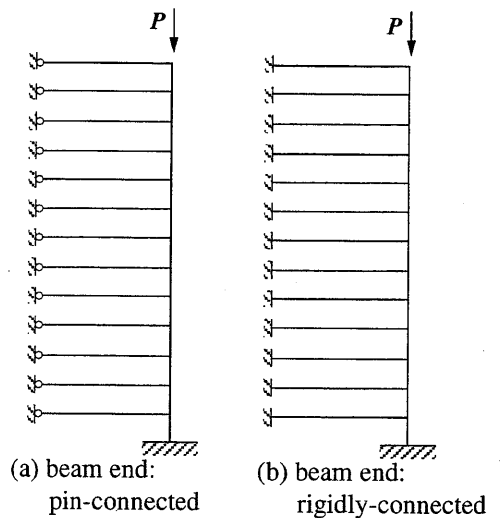


Fig. 5 Frame Models for Sidesway Prevented

ered, although the size of the coefficient matrix is $2mx2m$ or mxm , depending on the frame considered. The buckling load parameter Z_{cr} is determined from the condition that the determinant of the coefficient matrix of Eq. (28) becomes zero. In the numerical computation, a trial-and-error procedure was taken in the following manner. First, the elements of $[A]$ was computed for a trial value of Z , and an eigenvalue problem was set as follows:

$$[A] \{ X \} - \lambda \{ X \} = \{ 0 \} \tag{43}$$

Since the determinant of the matrix is given by the product of all eigenvalues, that is,

$$|[A]| = \lambda_1 \cdot \lambda_2 \cdot \lambda_3 \dots \lambda_N \tag{44}$$

where $N = 2m$ or m , it was checked whether an eigenvalue with the smallest absolute value changed the sign. If yes, a range for the existence of Z_{cr} was captured, and if not, another trial value for Z was set and the procedure was repeated. This procedure is actually more tedious and more time-consuming than the procedure of checking the change of sign of the determinant, but it is effective and safe to avoid missing the point of zero determinant, since the determinant does not change its sign, if even number of eigenvalues change their signs together in the case of the increment of the trial values for Z is too large. Analysis of the eigenvalues was carried out by the combination of QR and Householder's methods.

4. Results of Analysis

The buckling analysis was carried out for a number of sample model frames with the following parameters: i) the beam stiffness ratio $k = 2$, ii) the wall stiffness ratio $n = 1, 2, 10$ and 100 , and iii) the number of stories $m = m' = 3, 50$ and 100 .

4.1 Accuracy of Approximate Solution

(a) Constant Distribution of Stiffness and Load Parameter along the Height of the Frame

The buckling analysis was carried out for the model frame A, in which the stiffness ratios of the column, beam and wall, and the load parameter Z are all constantly distributed along the height of the frame. Table 1 shows the values of Z_{cr} , obtained by the approximate analysis shown in Chapter 2, and the exact analysis in Chapter 3, and the error that is defined as the ratio of the difference between the values of approximate and exact solutions to the value of the exact solution. The positive error indicates the approximate solution is higher than the exact solution.

The following characteristics are observed from the results shown in Table 1:

Table 1 Comparison of Z_{cr} Obtained by Approximate and Exact Analyses
Frame A: constant stiffness and load parameter

k	n	m	beam end: pin-connected			beam end: rigidly-connected		
			<i>approx.</i>	<i>exact</i>	<i>error</i>	<i>approx.</i>	<i>exact</i>	<i>error</i>
2	1	3	2.07	2.21	-0.06	3.40	3.52	-0.03
		50	1.98	1.98	-0.00	3.36	3.36	-0.00
		100	1.98	1.98	-0.00	3.36	3.36	-0.00
	2	3	2.12	2.28	-0.07	3.66	3.82	-0.04
		50	1.98	1.98	-0.00	3.59	3.59	-0.00
		100	1.98	1.97	0.01	3.59	3.59	-0.00
	10	3	2.47	2.71	-0.09	4.09	4.38	-0.07
		50	1.98	1.98	-0.00	3.84	3.84	0.01
		100	1.98	1.98	-0.00	3.84	3.84	-0.00
	100	3	4.88	4.60	0.06	5.67	4.81	0.18
		50	2.00	2.01	-0.00	3.91	3.93	-0.01
		100	1.98	1.99	-0.01	3.91	3.93	-0.00

k : beam stiffness ratio n : wall stiffness ratio m : number of story
error: (approximate solution - exact solution) / exact solution

- i) The accuracy of the approximate solution is very good, except for the case of 3-story frames.
- ii) The effect of wall stiffness ratio on the buckling strength clearly appears in the 3-story frames, and in the frames in which the beams are rigidly-connected to the wall, while the buckling strength of 50- and 100-story frames are not sensitive with the change in the wall stiffness ratio in the frames in which the beams are pin-connected to the wall. This tendency is observed in both approximate and exact solutions.
- iii) The buckling strength does not change with the number of story, if it is sufficiently large, that is, 50-story in the present numerical example.
- iv) The value of Z_{cr} of the 50- and 100-story frames in which the beams are pin-connected to the wall is smaller than π , and thus the effective column length is larger than the story height. The contrary is observed in the 50- and 100-story frames in which the beams are rigidly-connected to the wall, even in the case of small wall stiffness: the value of Z_{cr} is larger than π , and the effective column length is smaller than the story height.

(b) Linearly Varying Distribution of Stiffness and Load Parameter along the Height of the Frame

The buckling analysis was carried out for the model frame B, in which the stiffness ratios of the column, beam and wall, and the load parameter Z are all linearly varying along the height of the frame, with the following parameters: i) the parameter a , defining varying ratio of the column stiffness in Eq. (30), $a = 1/m$, and ii) the parameter κ , defining varying ratio of the load parameter in Eq. (32), $1/\kappa = 1.00, 1.01, 1.05, 1.10, 1.125$. The distributions of the beam and wall stiffness ratios are given by Eq. (31), which are similar to that of the column stiffness ratio.

Table 2 shows the values of Z_{cr} , obtained by the approximate and exact analyses, and the error. The values of the error are plotted against the values of $1/\kappa$ for various values of n in Fig. 6.

The following characteristics are observed from the results shown in Table 2:

- i) The accuracy of the approximate solution is very good, except for the case of 3-story frames. The value of $a = 1/m$ is too small, and such a steep variation of the member stiffness never occurs in the real building frames. This indicates that the approximate solution is applicable to the real case of more gentle variation of the stiffness.
- ii) Similar observations to those indicated in items ii) and iv) in the previous section are also made in the frames with linear variation of stiffness and load parameter.
- iii) A little difference is observed between the exact solution of Z_{cr} of 50- and 100-story frames, which is not observed in the frames with constant distribution of the stiffness and load parameter, and the difference becomes larger, as the wall stiffness ratio n increases.

Table 2.1 Comparison of Z_{cr} Obtained by Approximate and Exact Analyses
 Frame B: linearly varying stiffness and constant load parameter, $1/\kappa = 1.00$

k	n	m	beam end: pin-connected			beam end: rigidly-connected		
			<i>approx.</i>	<i>exact</i>	<i>error</i>	<i>approx.</i>	<i>exact</i>	<i>error</i>
2	1	3	2.07	2.31	-0.10	3.40	3.67	-0.07
		50	1.98	1.99	-0.01	3.36	3.37	-0.00
		100	1.98	1.98	-0.00	3.36	3.37	-0.00
	2	3	2.12	2.35	-0.10	3.66	4.01	-0.09
		50	1.98	1.99	-0.01	3.59	3.60	-0.00
		100	1.98	1.98	-0.00	3.59	3.60	-0.00
	10	3	2.47	2.64	-0.06	4.09	4.72	-0.13
		50	1.98	1.99	-0.01	3.84	3.86	0.01
		100	1.98	1.98	-0.00	3.84	3.85	-0.00
100	3	4.88	4.78	0.02	5.67	5.00	0.13	
	50	2.00	1.99	0.01	3.91	3.96	-0.01	
	100	1.98	1.98	-0.00	3.91	3.93	-0.01	

k : beam stiffness ratio n : wall stiffness ratio m : number of story
error: (approximate solution - exact solution) / exact solution

Table 2.2 Comparison of Z_{cr} Obtained by Approximate and Exact Analyses
 Frame B: linearly varying stiffness and load parameter, $1/\kappa = 1.01$

k	n	m	beam end: pin-connected			beam end: rigidly-connected		
			<i>approx.</i>	<i>exact</i>	<i>error</i>	<i>approx.</i>	<i>exact</i>	<i>error</i>
2	1	3	2.07	2.32	-0.11	3.40	3.69	-0.08
		50	1.98	1.99	-0.00	3.36	3.38	-0.01
		100	1.98	1.99	-0.00	3.36	3.37	-0.00
	2	3	2.12	2.36	-0.10	3.66	4.04	-0.09
		50	1.98	1.99	-0.00	3.59	3.62	-0.01
		100	1.98	1.99	-0.00	3.59	3.61	-0.00
	10	3	2.47	2.63	-0.07	4.09	4.75	-0.14
		50	1.98	1.99	-0.00	3.84	3.88	-0.01
		100	1.98	1.99	-0.00	3.84	3.86	-0.00
100	3	4.88	4.80	0.02	5.67	5.03	0.13	
	50	2.00	2.00	-0.00	3.91	3.98	-0.02	
	100	1.98	1.99	-0.00	3.91	3.94	-0.01	

k : beam stiffness ratio n : wall stiffness ratio m : number of story
error: (approximate solution - exact solution) / exact solution

Table 2.3 Comparison of Z_{cr} Obtained by Approximate and Exact Analyses
 Frame B: linearly varying stiffness and load parameter, $1/\kappa = 1.05$

k	n	m	beam end: pin-connected			beam end: rigidly-connected		
			<i>approx.</i>	<i>exact</i>	<i>error</i>	<i>approx.</i>	<i>exact</i>	<i>error</i>
2	1	3	2.07	2.34	-0.12	3.40	3.76	-0.10
		50	1.98	2.01	-0.01	3.36	3.40	-0.01
		100	1.98	2.00	-0.01	3.36	3.38	-0.01
	2	3	2.12	2.38	-0.11	3.66	4.12	-0.11
		50	1.98	2.01	-0.01	3.59	3.63	-0.01
		100	1.98	2.00	-0.01	3.59	3.61	-0.01
	10	3	2.47	2.69	-0.08	4.09	4.87	-0.16
		50	1.98	2.01	-0.01	3.84	3.91	-0.02
		100	1.98	2.00	-0.01	3.84	3.89	-0.01
100	3	4.88	4.86	-0.00	5.67	5.13	0.10	
	50	2.00	2.02	-0.01	3.91	4.05	-0.04	
	100	1.98	2.00	-0.01	3.91	3.99	-0.02	

k : beam stiffness ratio n : wall stiffness ratio m : number of story
error: (approximate solution - exact solution) / exact solution

Table 2.4 Comparison of Z_{cr} Obtained by Approximate and Exact Analyses
 Frame B: linearly varying stiffness and load parameter, $1/\kappa = 1.10$

k	n	m	beam end: pin-connected			beam end: rigidly-connected		
			<i>approx.</i>	<i>exact</i>	<i>error</i>	<i>approx.</i>	<i>exact</i>	<i>error</i>
2	1	3	2.07	2.38	-0.13	3.40	3.83	-0.11
		50	1.98	2.01	-0.02	3.36	3.41	-0.01
		100	1.98	2.00	-0.01	3.36	3.39	-0.01
	2	3	2.12	2.42	-0.12	3.66	4.21	-0.13
		50	1.98	2.01	-0.02	3.59	3.65	-0.02
		100	1.98	2.00	-0.01	3.59	3.63	-0.01
	10	3	2.47	2.73	-0.09	4.09	5.32	-0.23
		50	1.98	2.01	-0.02	3.84	3.94	-0.02
		100	1.98	2.00	-0.01	3.84	3.91	-0.02
	100	3	4.88	4.91	-0.01	5.67	5.24	0.08
		50	2.00	2.04	-0.02	3.91	4.11	-0.05
		100	1.98	2.00	-0.01	3.91	4.04	-0.03

k : beam stiffness ratio n : wall stiffness ratio m : number of story
error: (approximate solution - exact solution) / exact solution

Table 2.5 Comparison of Z_{cr} Obtained by Approximate and Exact Analyses
 Frame B: linearly varying stiffness and load parameter, $1/\kappa = 1.125$

k	n	m	beam end: pin-connected			beam end: rigidly-connected		
			<i>approx.</i>	<i>exact</i>	<i>error</i>	<i>approx.</i>	<i>exact</i>	<i>error</i>
2	1	3	2.07	2.39	-0.13	3.40	3.85	-0.12
		50	1.98	2.01	-0.02	3.36	3.42	-0.02
		100	1.98	2.00	-0.01	3.36	3.40	-0.01
	2	3	2.12	2.43	-0.13	3.66	4.25	-0.14
		50	1.98	2.01	-0.02	3.59	3.66	-0.02
		100	1.98	2.00	-0.01	3.59	3.63	-0.01
	10	3	2.47	2.75	-0.10	4.09	5.07	-0.19
		50	1.98	2.03	-0.02	3.84	3.95	-0.03
		100	1.98	2.00	-0.01	3.84	3.90	-0.02
	100	3	4.88	4.92	-0.01	5.67	5.28	0.07
		50	2.00	2.03	-0.01	3.91	4.15	-0.06
		100	1.98	2.01	-0.02	3.91	4.05	-0.03

k : beam stiffness ratio n : wall stiffness ratio m : number of story
error: (approximate solution - exact solution) / exact solution

The following characteristics are observed from the results for 50- and 100-story frames shown in Fig. 6:

- i) The error linearly increases, as the value of $1/\kappa$ increases.
- ii) In the case of frames in which the beams are pin-connected to the wall, 4 lines indicating the errors in the frames with 4 values of the wall stiffness ratio n become almost identical.
- iii) The error in the 100-story frames is generally smaller than those in the 50-story frames.
- iv) The largest error appears in the 50-story frames with $n = 100$ in which the beam ends are rigidly-connected to the wall.
- v) Within the limitation of $1/\kappa \leq 1.125$, the error is within 5 %, except one case, that is, $m = 50$, $n = 100$ and $1/\kappa = 1.125$.

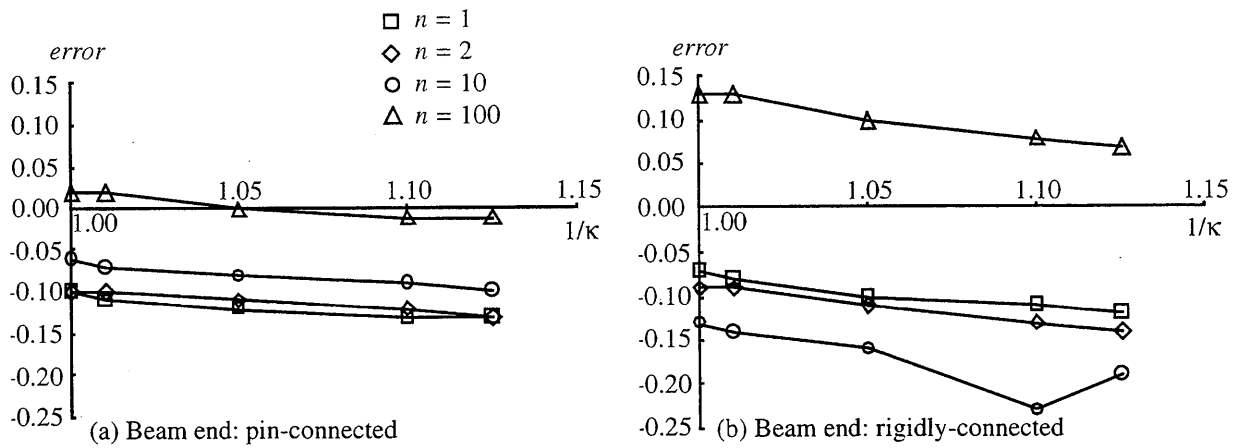


Fig. 6.1 Variation of Error with n and κ : $m = 3$

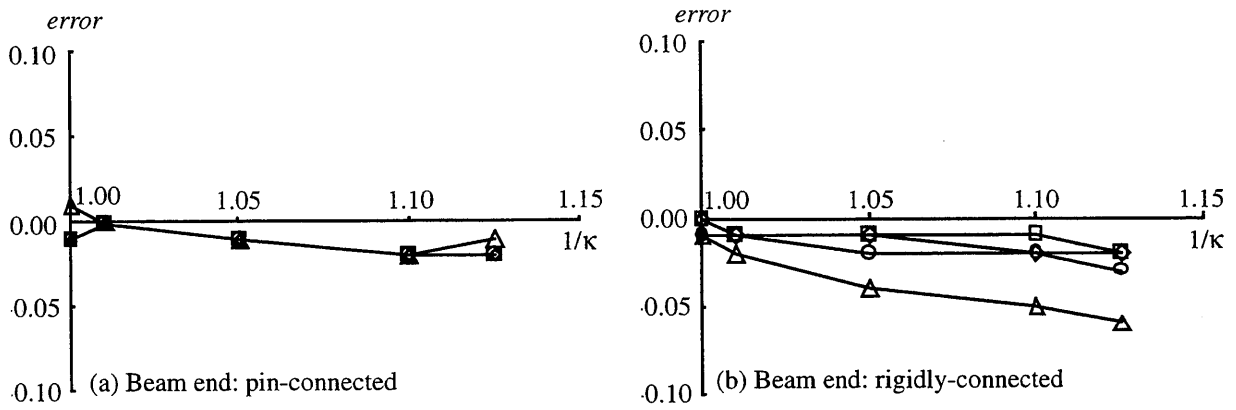


Fig. 6.2 Variation of Error with n and κ : $m = 50$

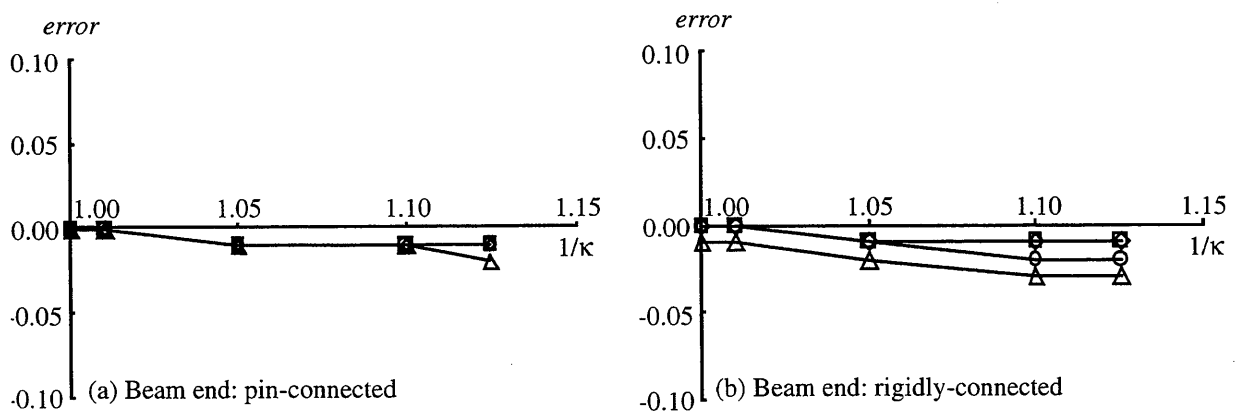


Fig. 6.3 Variation of Error with n and κ : $m = 100$

4.2 Alignment Chart

The numerical results of the buckling analysis of the model frame B shown in Table 2 and Fig. 6 conclude that the approximate method of analysis is applicable to tall buildings, but not to low-rise frames such as the 3-story frame. The accuracy of the approximate solution has been investigated from the numerical results of the buckling analysis of the model frame A with $k = 2$ and $n = 10$ by changing the number of story m , and it is revealed that the value of Z_{cr} does not change much and the error is very small, if the value of m is not less than 30. Then, the approximate values of Z_{cr} have been calculated for the model frame A with $m = 30$, by changing the beam stiffness ratio k and the wall stiffness ratio n , and the alignment charts shown in Fig. 7 are obtained. These charts are applicable to a general frames in which the beam ends are pin- or rigidly-connected to the wall, with the limitation of $m \geq 30$ and $1/\kappa \leq 1.125$.

4.3 Effect of Sidesway

Eigenvalue analysis was carried out for the case that the sidesway of each story was assumed to be completely prevented. Table 2 compares the exact solutions obtained by the eigenvalue analysis for the frames with the sidesway permitted (model frame A) and prevented (model frame C). The error is defined as the ratio of the difference between the buckling strengths for the frames with the sidesway permitted and prevented to the strength with the sidesway permitted.

Note the following points from the results shown in Table 2:

- i) The difference in the buckling strength between the sidesway permitted and prevented is very large, even in the case of the wall stiffness ratio equal to 100, except for the 3-story frame. This indicates that the effect of sidesway cannot be neglected in the case of tall buildings, even though it is connected to a structural wall with large lateral stiffness.
- ii) The buckling strength does not change with the number of story, if it is sufficiently large, regardless of the sidesway condition.
- iii) In the case of the sidesway-prevented frames with the beam ends pin-connected, the wall stiffness does not affect the buckling strength.

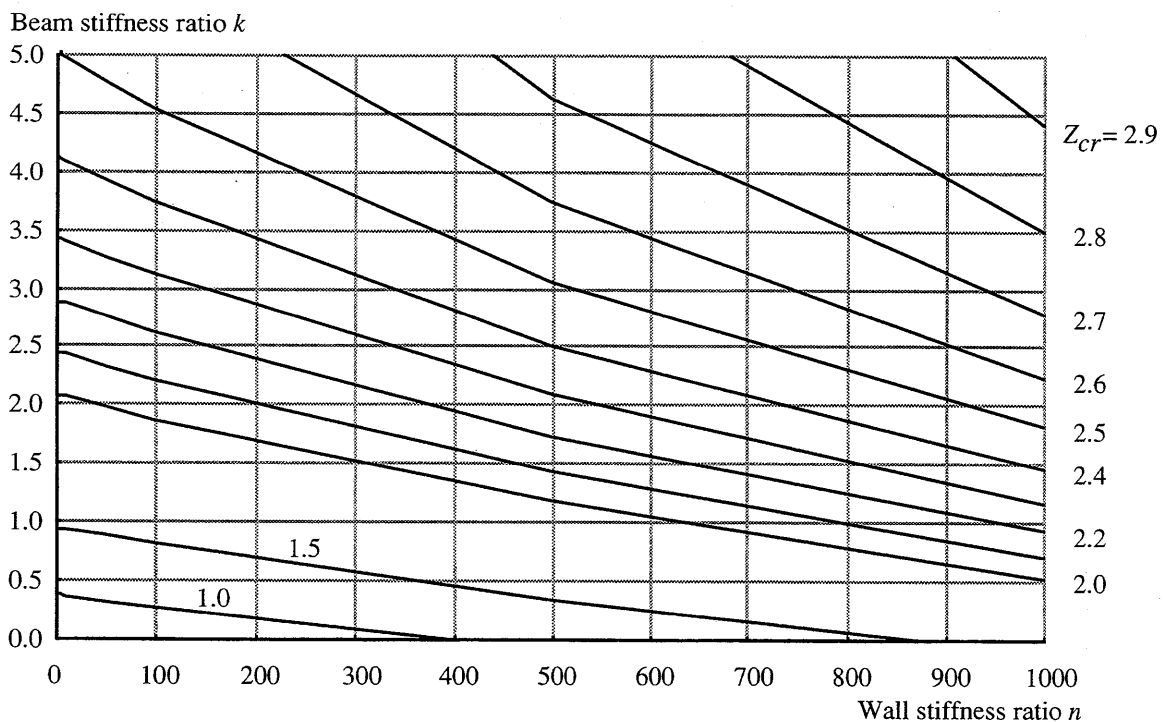


Fig. 7(a) Alignment Chart for the Frames with Beam Ends Pin-Connected

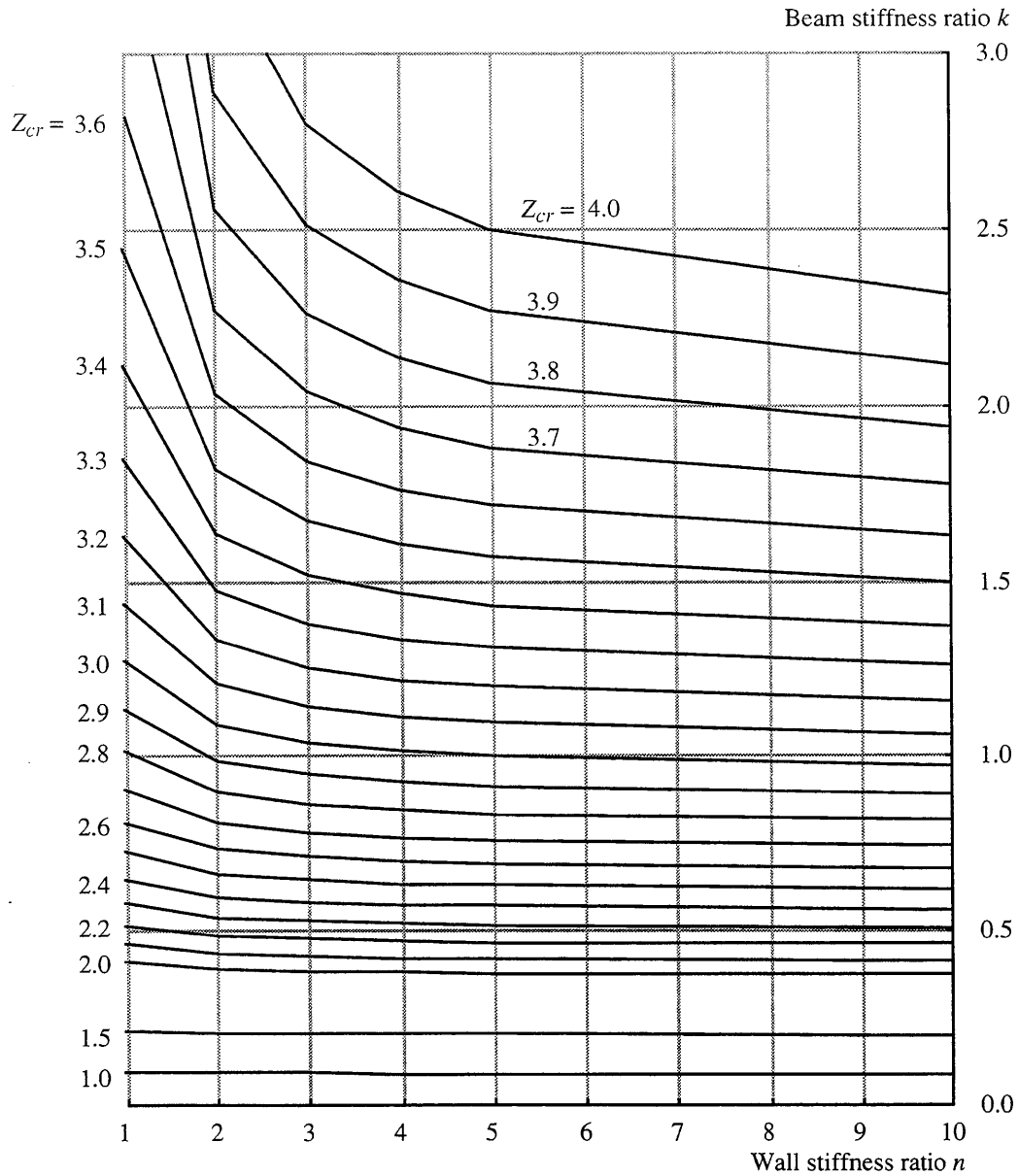


Fig. 7(b) Alignment Chart for the Frames with Beam Ends Rigidly-Connected

Table 3 Comparison of Z_{cr} for Sidesway-Permitted and Prevented Frames
Frames A and C: constant stiffness and load parameter

k	n	m	beam end: pin-connected			beam end: rigidly-connected		
			sidesway permitted	sidesway prevented	error	sidesway permitted	sidesway prevented	error
2	1	3	2.21	4.61	-1.08	3.52	4.69	-0.33
		50	1.98	4.35	-1.20	3.36	4.43	-0.32
		100	1.98	4.35	-1.20	3.36	4.43	-0.32
	2	3	2.28	4.61	-0.21	3.82	4.72	-0.24
		50	1.98	4.35	-1.20	3.59	4.47	-0.25
		100	1.97	4.35	-1.21	3.59	4.47	-0.25
	10	3	2.71	4.61	-0.70	4.38	4.79	-0.09
		50	1.98	4.35	-1.20	3.84	4.54	-0.18
		100	1.98	4.35	-1.20	3.84	4.54	-0.18
	100	3	4.60	4.61	-0.00	4.81	4.82	-0.00
		50	2.01	4.35	-1.16	3.93	4.58	-0.17
			100	1.99	4.35	-1.19	3.91	4.58

k : beam stiffness ratio n : wall stiffness ratio m : number of story
 error: (sidesway permitted - sidesway prevented) / sidesway permitted

4. Concluding Remarks

A method of approximate analysis was proposed for the buckling strength of single-bay multi-story steel frames connected to a core wall. The solution was obtained by a simple and easy computation. It was shown that the accuracy of the approximate solution was very good, compared with the exact solution obtained by the eigenvalue analysis for several sample tall frames. Alignment charts for the effective column length were prepared, which are applicable to the frames in which the beams are pin- or rigidly-connected to the wall, with the limitation that the number of story of the frame should be not less than 30, and the inverse value of the parameter κ defining varying ratio of the load parameter Z should be not larger than 1.125.

The frame model treated in this paper is a single-bay frame as shown in Fig. 1, while the real frame has multi-bays. The buckling strength of the frame consisting of a steel beam-and-column assembly with s -bays (s columns) connected to a core wall may be obtained by breaking down the given frame to a series of s single-bay frames of the type shown in Fig. 1. The effectiveness of this procedure is left for the future investigation.

References

- Bleich, H. H. (1951). "Buckling Strength of Metal Structures", McGraw-Hill Book Company, Inc., New York.
- Cheong-Siat-Moy, F. (1978). "Frame Design without Using Effective Length", *Journal of the Structural Division, Proceedings of the American Society of Civil Engineers*, 104(1), 23-33.
- Chu, K. H. and Chou H. L. (1969). "Effective Length in Unsymmetrical Frames", *Publications of International Association for Bridge and Structural Engineering*, 29-1, 1-15.
- Lind, N. C. (1977). "Simple Illustration of Frame Instability", *Journal of the Structural Division, Proceedings of the American Society of Civil Engineers*, 103(1), 1-8.
- Morino, S., Kawaguchi, J. and Suzuki, H. (1993). "Approximate Method of Elastic Buckling Strength Analysis for Irregular Frames", *Research Report, Faculty of Engineering, Mie University*, 18, 59-72.
- Sakamoto, J. (1980). "Guide to Stability Design of Steel Structures, First Edition, Chapter 15 Frame Stability" *Architectural Institute of Japan, Tokyo (in Japanese)*.
- Wood, R. H. (1974). "Effective Length of Columns in Multi-Story Buildings", *The Structural Engineer*, 52, 235-244.